Self-assembly of a phospholipid Langmuir monolayer using coarse-grained molecular dynamics simulations

2002 J. Phys.: Condens. Matter 14 9431

(http://iopscience.iop.org/0953-8984/14/40/327)

INSTITUTE OF PHYSICS PUBLISHING JOURNAL OF PHYSICS: CONDENSED MATTER

J. Phys.: Condens. Matter **14** (2002) 9431–9444 PII: S0953-8984(02)36747-X

Self-assembly of a phospholipid Langmuir monolayer using coarse-grained molecular dynamics simulations

Carlos F Lopez[1], **Steve O Nielsen**[1], **Preston B Moore**[1], **John C Shelley**[1,2] **and Michael L Klein**[1,3,4]

[1] Center for Molecular Modeling and Department of Chemistry, University of Pennsylvania, 231 S 34th St Philadelphia, PA 19104-6323, USA
[2] Schrödinger Inc., 1500 S W First Ave., Suite 1180, Portland, OR 97201, USA

E-mail: klein@cmm.upenn.edu

Received 9 May 2002
Published 27 September 2002
Online at stacks.iop.org/JPhysCM/14/9431

Abstract

Molecular dynamics simulations using a coarse-grained (CG) model for dimyristoyl-phosphatidyl-choline and water molecules have been carried out to follow the self-assembly process of a Langmuir monolayer. We expand on a previous study of the characteristics of the CG model where we compare the rotational and translational constants of the present model to those of an all-atom (AA) model, and find that the rotational and translational timescales are up to two orders of magnitude faster than in an AA model. We then apply the model to the self-assembly of a Langmuir monolayer. The initial randomly distributed system, which consists of 80 lipids and 5000 water sites, quickly self-assembles into two Langmuir monolayers and a micelle in the bulk water region. The micelle slowly diffuses towards and fuses with one of the interfacial monolayers, leaving the final equilibrated state with a Langmuir monolayer at each of the two air/water interfaces. The effective speed-up gained from the CG approach gives access to timescales and spatial scales that are much larger than those currently accessible with AA models.

(Some figures in this article are in colour only in the electronic version)

1. Introduction

Physical properties of lipid bilayers have been studied extensively [1, 2], exploring such features as membrane dynamics and structural and dynamical aspects of membrane–protein interactions [3]. The timescales of motion of lipid membranes span many orders of magnitude

[3] Author to whom any correspondence should be addressed.
[4] www.cmm.upenn.edu

0953-8984/02/409431+14$30.00

from intra-molecular bond vibrations at the femtosecond level (10^{-15} s), to lipid trans-bilayer flips at the second (10^{0} s) timescale [2]. A range of timescales have been studied by different methods such as NMR and IR techniques [1], as well as by computer simulation [4–6]. However, a gap in the study of membranes exists between the molecular-scale events at the atomic level and the macroscopic behaviour. It is here, at the mesoscale level spanning spatial scales of hundreds of nanometres to microns and temporal scales of hundreds of nanoseconds to milliseconds, where we are focusing our efforts to gain understanding of the physics that governs processes such as membrane fission, fusion, and domain formation, as well as mesoscopic interactions with proteins.

It is widely recognized that, rather than behaving as an inert medium in which proteins are embedded, biological membranes display a rich variety of dynamical phenomena, from thermal fluctuations such as undulatory and peristaltic modes, to activated processes such as raft formation and protein aggregation [7]. In order to study such systems in the mesoscale regime with computer simulations it is necessary to make some compromises compared to the atomistic models. We formulate a representation of the lipid membrane in which some of the detailed structure is captured in an implicit or average manner while a description of the chemical attributes of the molecules is maintained. One would aim at studying the mesoscopic properties of a membrane without losing sight of events that carry a significant weight at the molecular level. With this motivation a coarse-grained (CG) model for lipids and water has been developed to study such events.

Drawing on reverse Monte Carlo simulation techniques [8, 9] we have described a procedure [10] for constructing a reduced model of a lipid system. The construction relies on having an accurate short-time atomistic molecular dynamics (MD) simulation which is used to calibrate the model. The aim of the material presented in the main body of the paper is twofold. Firstly, for both the bilayer and Langmuir monolayer systems, we extend our previous CG studies [10, 11] by further characterizing the dynamical properties of the lipid. Secondly, in the main focus of the present work, we explore new ground by studying the fusion of a micelle with a membrane in the self-assembly process of a Langmuir monolayer. In passing, we present a comparison of the translational and rotational diffusion timescales between an all-atom (AA) model [12] and the present CG model.

2. Methods

2.1. Coarse-grained model

The CG model employs simplified representations for the lipid and water molecules as described thoroughly in previous work [10, 11, 13]. We construct models of lipids and water that mimic structural and physical features known from experimental or AA simulation results. Single spherical sites represent groups of atoms. These sites are then linked using stretching and bending potentials to obtain a representation of a lipid which preserves the rough shape of the molecule. Water sites are parametrized to represent three water molecules. The present results utilize modified parameters that can handle simulations in the NPT ensemble [14].

The CG model for dimyristoyl-phosphatidyl-choline (DMPC) is shown in figure 1. The CH site represents the choline part of the head group while the PH site represents the phosphate entity. The GL, E1, and E2 sites represent the central glycerol atoms and the ester carbons respectively. Notice the difference in distance between E2 and GL and E1 and GL emphasizing the fact that the tails have different lengths in the AA lipid. The SM sites represent three methylene groups, while the ST sites represent two methylene groups and a terminal methyl group.

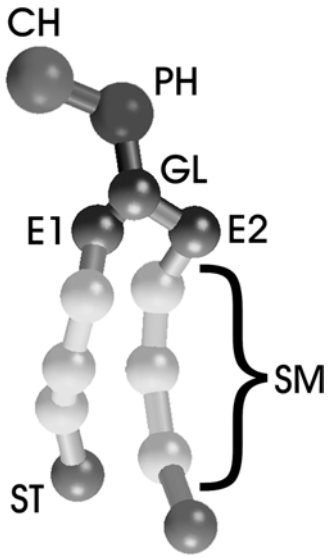

Figure 1. CG representation of DMPC. The choline (CH), phosphate (PH), ester groups (E1, E2), glycerol (GL), chain methyl (SM), and terminal methyl (ST) units are shown and labelled.

We have previously shown [11] that enhanced diffusion due to the soft interaction potentials leads to an effective speed-up of about two orders of magnitude over the actual simulation time. In addition to this, there is a net gain from the simulation due to the reduction of interaction sites as will be discussed later.

2.2. Simulation systems

An equilibrated 64-DMPC lipid bilayer using the model described above was taken from a previous run and replicated 16 times to construct a lipid bilayer with 1024 DMPC molecules and 8768 water sites. This corresponds to about 26 water molecules per lipid; at 303.15 K this should correspond to a bilayer system in the L_α phase. This lipid bilayer was then equilibrated in the constant-volume and constant-temperature (NVT) ensemble for 10 ps, which corresponds roughly to 1 ns of effective dynamics. The production run consisted of 800 ps of dynamics in the constant-pressure and constant-temperature (NPT) ensemble, at 303.15 K and 1 atm, in an orthorhombic unit cell. This run effectively corresponds to 80 ns of real dynamics of the lipid bilayer. The temperature and pressure were controlled using the Nosé–Hoover formalism [15, 16]. A chain length of 4 was used for the thermostat. Three-state multiple-time-step integration using the RESPA algorithm was used to integrate the equations of motion [17]. The shortest steps, 1 fs, were used for bond-length and bond-angle integration, while the intermediate steps, 2 fs, were used for non-bonded interactions less than 11 Å. The long steps, 40 fs, were used for non-bonded interactions between 11 Å and the cut-off. The van der Waals cut-off was set at 15 Å. The long-range electrostatic interactions are not truncated but rather treated with Ewald sums.

The main part of our study consisted of a simulation of the self-assembly of a Langmuir monolayer. The same model as described above was used for the lipid and water molecules. A slab with three-dimensional periodic boundary conditions, with dimensions 70 Å for the x- and y-direction and 400 Å in the z-direction was built. To emulate an air–water interface, we initially restrict molecules to a 140 Å slab in the z-direction. With the present set-up the

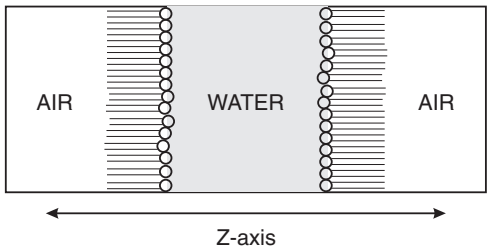

Figure 2. Schematic representation of a Langmuir monolayer set-up in a MD simulation. The lipid head groups (circles) point toward the bulk water region in the centre of the slab. The tails of the lipid point towards the air side on the edges.

system has two vacuum–water interfaces with a common water slab in the middle as depicted in figure 2. The interactions of the monolayers are minimized by placing enough water between them.

The system was started from a random configuration as follows. A single lipid configuration and a single water configuration were generated. A set of three Euler angles and three spatial coordinates were chosen to be independently and uniformly random over their full range. The single lipid was rotated and displaced by this set of variables 80 times to generate a random placement of 80 lipids in the slab. Additionally, a set of 5000 spatial coordinates were drawn and applied to the single water configuration to generate 5000 randomly placed water particles in the slab. Euler angles are not needed for the water since it lacks internal structure [10]. Bad contacts were removed by short MD runs. A single production run was then launched in the NVT ensemble at 303.15 K.

The production run for the self-assembly consisted of 100 000 steps of dynamics for a total time of 2 ns, corresponding to an effective simulation time of about 200 ns. This production run took less than one week on a single 1.4 GHz Intel Pentium IV® processor.

3. Results and discussion

The spirit of the CG approach is to minimize the number of variables necessary to describe a system without losing a useful description of the system. This approach is helpful in a context where relatively large collective motions are necessary to explore a system's properties: specifically, when either the system is too large or the events under investigation are too slow for an all-atom simulation. Due to the necessary simplifications and averaging involved in the creation process of a CG model, some of the physical properties are not reproduced at the same level of accuracy as with an AA approach. It is therefore important to understand the advantages and limitations of the present CG model. The time units used for figures and discussion in this work are reported without scaling for the enhanced diffusion of the particles, which, as mentioned above, is up to two orders of magnitude larger than those reported. When considering the overall dynamics of the processes described herein, the reader should be aware that the general scale of the events is two orders of magnitude larger.

3.1. Coarse-grained simulation of a 1024-DMPC lipid membrane

3.1.1. Membrane properties. Being able to relate both dynamical and structural features of the CG membrane to those determined by atomistic simulation methods or experiments is essential for applications of the present CG model. For this reason one must calibrate the model

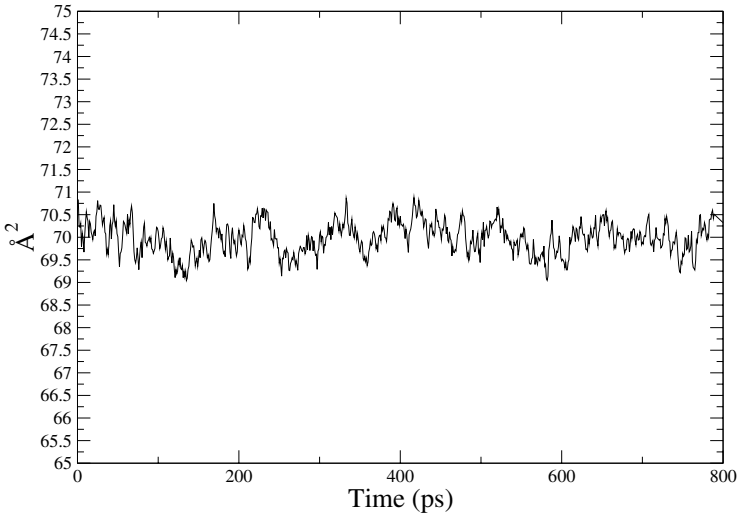

Figure 3. Time evolution of the area per head group in a CG 1024-DMPC lipid bilayer simulation. The area per head group remains essentially constant throughout the run.

to match or reproduce trends in the AA simulation. Properties such as area per head group and bilayer thickness are of structural importance and we aim to be consistent with measurements of these quantities. The bilayer thickness for the AA simulation is 36 Å [12] while that for the CG model is 32 Å [11]. The area per head group in the AA model, using the AMBER force field [12], is 58 Å^2, while that for the CG model is 70 Å^2 [11]. The experimental value for the area per head group ranges from 59.5 to 67.6 Å^2 depending on the method employed and the experimental conditions; the latest value reported by Nagle and co-workers [18] is 59.6 Å^2. The bilayer thickness is in good agreement with the corresponding values from AA simulation but the area per head group is about 20% off the AA value. This discrepancy could be due to the larger diameter of the tail sites, which are more like DPPC [19], and the overall difference in flexibility caused by the lipid tails. The parametrization of the CG could probably be improved to achieve a better match of the AA and experimental results, but is good enough for the present study. We are also interested in the long-time behaviour of the area per head group, as this can be an important factor when studying thermal fluctuations at the membrane–water interface. We plot the area per head group throughout the simulation in figure 3. It is evident from this plot that the area per head group remains stable throughout the run and the fluctuations are no more than 1 Å^2 from the mean. Given that the simulation is run in the NPT ensemble, it should be noted that these fluctuations will be related to temperature and pressure changes.

3.2. Membrane dynamics

3.2.1. Translational properties of the lipid. The main goal of the present CG approach is to investigate larger systems at longer timescales. Current AA simulations typically span 10 ns of simulation time with 10^4–10^5 atoms. Larger systems have been reported but some simplifications were necessary to make the problem computationally tractable [20]. It has been shown that using electrostatic cut-offs can alter the dynamic properties of the system [21–27]. Structural properties such as area per head group and bilayer thickness are generally conserved, but dynamical properties such as diffusion are generally altered when electrostatic cut-offs are

implemented in the dynamics run. Due to the presence of charged species at the lipid head groups and to eliminate the possibility of errors in transport properties due to truncation, we do not cut off electrostatic interactions but rather treat them with Ewald sums. Ewald sums are not important for the treatment of water in our model since partial charges are not included within water sites. The model was parametrized, however, from an AA simulation that included full electrostatics through the Ewald sum methods. In the CG spirit, we try to capture the full electrostatic effects for water in an average manner through the use of mean-field tabulated potentials which are implemented as described in previous work [10, 13]. For the lipid head groups, however, the inclusion of dipolar charges is a better approximation for the present CG model than the alternative elimination of these charges. The charges are therefore included and treated with the Ewald sum algorithm.

The use of soft potentials and a reduced numbers of interaction sites makes it worthwhile to get an idea of the effective timescales that are being accessed by the CG lipid molecules. We compare the two-dimensional diffusion coefficient of the CG model and the AA model by obtaining the diffusion coefficient (D) from the limiting slope given by

$$D = \lim_{t\to\infty} \frac{1}{2d_f} \frac{\mathrm{d}}{\mathrm{d}t} \langle |r_i(t) - r_i(0)|^2 \rangle \tag{1}$$

where d_f is the number of dimensional degrees of freedom in the system and $r_i(t)$ is the centre-of-mass position of particle i at time t. We use equation (1) with $d_f = 2$ to estimate the lateral diffusion coefficient in the plane of the bilayer (the xy-plane).

The results obtained from this comparison are presented in figure 4. It can be seen from this figure that while the lipid molecules in the AA model are still approaching the hydrodynamic limit, the CG lipid molecules exhibit a constant slope past 100 ps. The slopes yield self-diffusion coefficients of $D_{AA} = 6.5 \times 10^{-8}$ cm^2 s^{-1} and $D_{CG} = 6.3 \times 10^{-6}$ cm^2 s^{-1} for the AA and CG models, respectively. The translational dynamics of the lipids in the CG model is therefore about two orders of magnitude faster than that in the AA model.

The total speed-up in the CG model comes from the combination of an increase in diffusion by the particles in addition to the reduced time that the calculation takes on the computer. The calculation of forces between molecules is reduced by about two orders of magnitude (118 atoms for AA versus 13 for CG) and the time step has also been increased by an order of magnitude. The combination of these increases with the faster diffusion of particles results in a sampling of dynamics at a much faster timescale. Therefore, an optimistic assessment of the accessible timescales with the CG model, using the present treatment of charged species, is up to five orders of magnitude larger in the diffusion ($100 \times 10 \times 100 = 10^5$) than an equivalent AA simulation with Ewald sums.

3.2.2. Rotational properties of the lipid. Continuing with dynamic properties of the lipid molecules we now look at the rotational diffusion. To do so, we must first define a molecular fixed reference frame. The principal axes of the moment-of-inertia tensor (MIT) allow the rotations of the molecule to be quantified (see figure 5). We project the xy-components of the MIT onto the xy-plane to examine the overall molecular rotation, and the projection of the z-component of the MIT onto the xy-plane is used to examine the overall wobble. In addition, we investigate the molecular rotation using the different vectors shown in figure 5: the PN vector links the PH unit to the CH unit (as defined in figure 1), while the SM (ST) vector is drawn from second SM (terminal ST) unit in one tail to its counterpart in the other tail.

Once these vectors are defined we can characterize their rotational motion by estimating the self-diffusion coefficient D_{rot}, given by the slope of the average mean square displacement (MSD) at long enough times. The self-diffusion coefficient is defined in equation (1). The

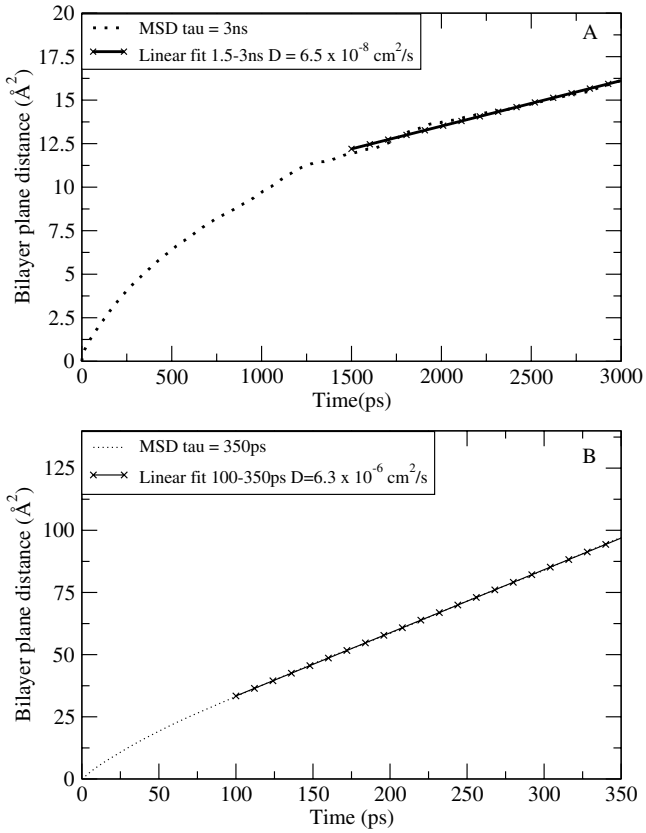

Figure 4. Two-dimensional MSD for a 10 ns AA DMPC simulation (A) and an 800 ps CG DMPC simulation (B). The fits are represented by the lines with crosses.

r-variable is changed to the angular θ-variable, which is defined as the angle after projection onto the xy-plane of one of the defined vectors with the x-axis.

The rotational self-diffusion coefficients for a DMPC all-atom lipid were determined previously [12] and are used here to compare the rotational timescales of the CG model with those of the AA model. Figure 6 shows the plot of the MSD of the individual vectors and the curves from which the diffusion coefficients are calculated.

The qualitative ordering of the rotational timescales is somewhat preserved in the CG model when compared to the AA model except for D_{rot} for the PN vector. The rotational scaling between the AA and CG models displays a broad range of differences. This is not overly worrisome since the overall internal dynamics of the molecules will be altered when compared to the AA molecules due to the lack of interactions and tangling that will occur in the AA description of a lipid. The value that merits closer discussion is that for D_{rot} for the PN vector. In the CG model the PN vector rotates the fastest, with $D_{rot} = 199$ rad^2 ns^{-1}. The PN vector in the CG model rotates much more freely than that of the AA simulation for the following reasons. In the AA simulation the zwitterionic head groups form a hydrogen bonding network with both water molecules and other lipids. This hydrogen bonding network must be broken in order for the head groups to rotate. In the CG model, however, the detailed hydrogen bonding network between water and head group as well as head group and head

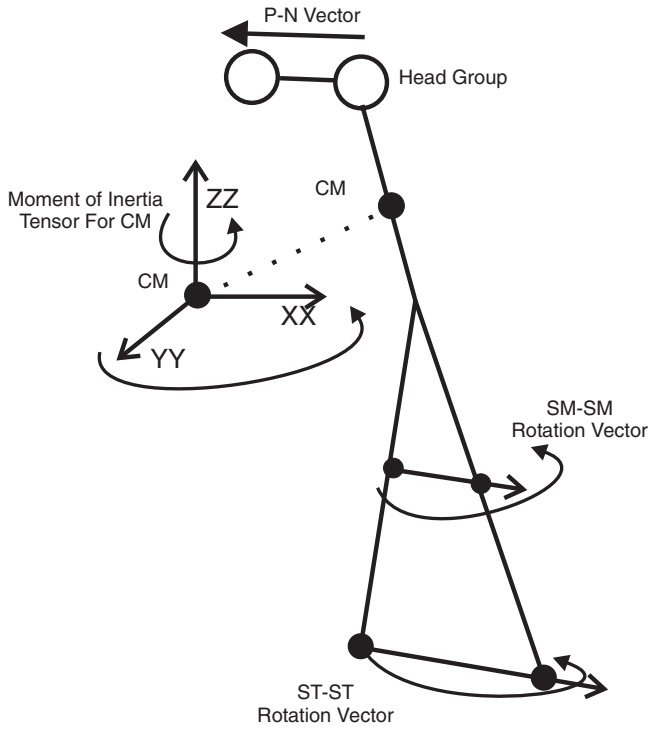

Figure 5. An illustration of the various vectors chosen to study rotational dynamics of DMPC. The vectors are defined and described in the text.

group has been captured in a statistical manner by the use of effective potentials. The resulting potential energy interaction therefore has reduced dynamical significance. It is important to note here that the average angle of the PN vector with the bilayer normal is about 90° (i.e. flat on the interface), which is in fair agreement with the AA value of about 76° (slight tilt off the interface) reported previously [12].

The two tail vector diffusions are roughly equal for the CG model, while those for the AA simulation differ by about an order of magnitude. This is expected, however, because in the CG model there are only four sites in the tail while the AA model has fourteen carbon atoms with their respective hydrogen atoms. In the AA model the long hydrocarbon tails tend to tangle and interact extensively making the rotations of the tails very slow when compared to the rotations of the rest of the molecule. In the CG model, the tail and molecular construct rotate as one unit.

The overall timescale ordering is preserved and the overall rotation is about an order to two orders of magnitude faster than in the AA simulation. This increase in rotational motion is in agreement with the previous section, where the two-dimensional translational diffusion coefficient of the CG model was found to be two orders of magnitude faster than the AA simulation. It is evident from the discussion so far that it can be difficult to capture all the properties of the lipid with a CG construct. We aim, however, to capture the major details that will influence the mesoscale behaviour of a bilayer or monolayer during the coarse-graining process, and, as seen thus far, we capture structural and some dynamic data effectively. The intrinsic motions of the lipid molecules will be more difficult to reproduce without including more terms or more sites into the model, although research is currently under way.

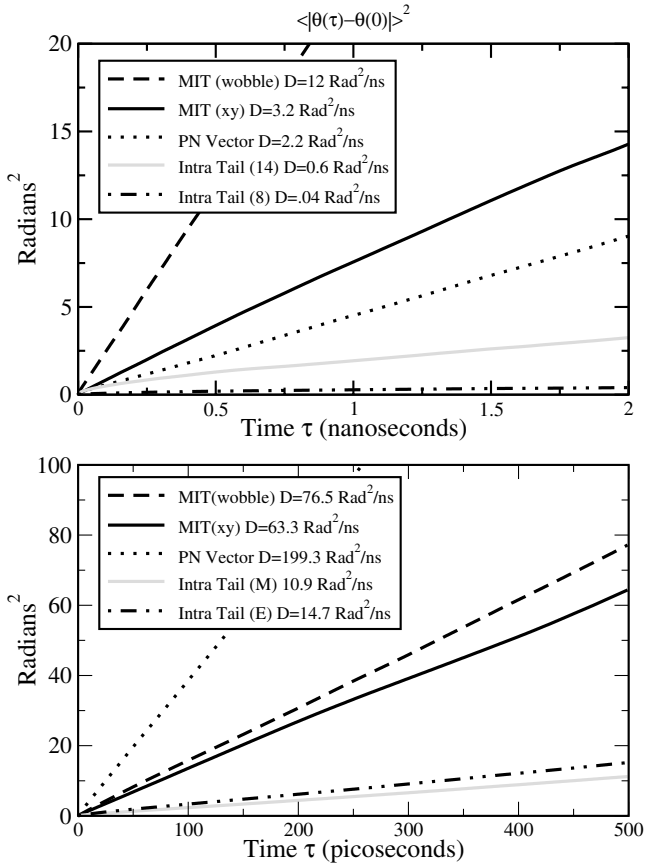

Figure 6. Comparison of the rotational diffusion between an AA simulation (top) and the CG lipid simulation (bottom). The plots are of MSDs of the vectors illustrated in figure 5. The D_{rot}-values are based on equation (1) as discussed in the body of the text.

3.3. Self-assembly of a monolayer

3.3.1. Self-assembly process. The self-assembly of randomly placed molecules into their expected thermodynamic phase is both difficult and time consuming with typical AA simulations. Taking advantage of the timescale speed-up and reduced number of interaction sites in the CG model, it has now become possible to study such processes. The self-assembly of a CG 64-DMPC lipid bilayer was reported previously [11] and its final structure was characterized. Here, we present the results of self-assembly of randomly placed lipids into a Langmuir monolayer as shown in figure 7.

Initially, the inhomogeneities that are present in the random initial placement of molecules give rise to local organization as the lipid tails try to remove their contacts with water. Very quickly these local aggregates accumulate either in a micelle in the bulk water region or as Langmuir monolayers at either of the two air/water interfaces (figure 7(B)). Although the precise number of lipids in each of these three entities will vary with the particular random placement initially chosen, this tripartite segregation was always observed over several simulations involving differing numbers of lipids (80 to 200 lipids) and using different random number seeds (data not shown). The self-assembly, structure, and dynamics of lipids in micelles

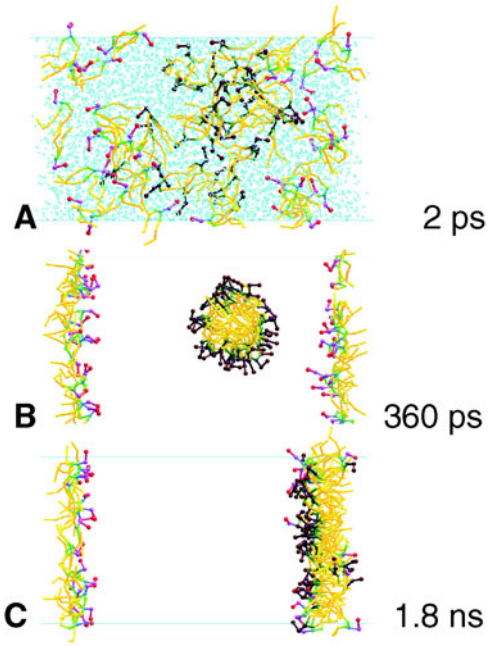

Figure 7. Snapshots of the evolution of the self-assembly of a random configuration of lipids into two monolayers at the air–water interface. Lipids with darker coloured head groups become part of the micelle while the lipids with lighter head groups form the initial monolayers. The initial configuration of the system is random as shown in panel A (waters shown). The simulation rapidly evolves to a configuration with two monolayers and a micelle and water (not shown) in the bulk (panel B). The micelle then diffuses towards the monolayer on the right and fuses with it towards the end of the MD run (panel C).

has been studied previously by different groups [28–30]. However, we focus herein on the fusion of the micelle and study the subsequent formation of a monolayer in the following section.

The micelle (a cylindrical micelle in the present case) could initially find itself far removed from the interfacial monolayer in a bulk water environment, or it could form close enough to the interface to immediately interact with one of the interfacial monolayers. In the former case the micelle will diffuse as an entity in bulk water—since it sees an isotropic bulk water environment it will diffuse randomly until at some point it drifts close enough to an interface to interact with one of the monolayers. This interaction can be thought of, at far enough separation, as the interaction between two amphiphilic surfaces [31]. In the case of the zwitterionic DMPC lipid there is no electric 'double layer' and it is observed that the micelle eventually fuses with the interfacial monolayer (figure 8) [31]. The process of both micelle diffusion and fusion with the monolayer are long-timescale events (compared to AA simulations)—well suited for investigation using the CG approach.

Perhaps the most interesting result from this investigation is the fusion of the micelle with the interfacial monolayer, which merits further discussion. Figure 9 shows the time evolution of the lipid head group density projected normal to the air/water interface. Of particular interest is the micellar fusion event and the bimodal density distribution that persists in the interface afterwards. Most of the lipids, both in the micelle and the monolayer, have time to reorient and displace during the fusion event.

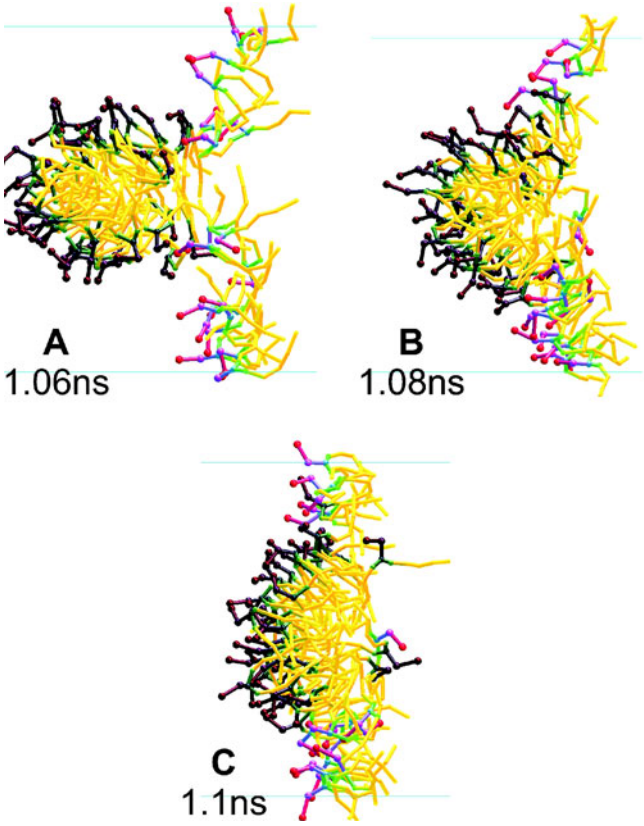

Figure 8. The fusion of the micelle with the monolayer. In panel A the monolayer has parted due to the proximity of the micelle. Panel B shows a snapshot shortly after fusion has begun. Notice that some lipids are ejected towards the outer surface during the collision. Panel C shows the micelle close to the end of the fusion event. Most head groups have aligned facing the water, while some lipids form a partial outer leaflet.

The monolayer lipid head groups evacuate the region near the incoming micelle. As the micelle approaches the interface, there is a depletion of monolayer head groups at the site of fusion. The micellar lipids closest to the monolayer, which are initially oriented in the opposite direction to the monolayer lipids, also have their head groups removed from this region (see figure 8(A)). The fusion process is a 'violent' event causing some lipids to be displaced towards the outer vacuum subphase of the monolayer (figures 8(B) and (C)). After the fusion event a steady-state population is seen to have been established in which a few of the lipids populate a partial bilayer leaflet. Individual lipids exchange between the water subphase and the vacuum subphase leaflets but the population in each leaflet is constant on average. The total number of lipids present at this interface is 59, which is a larger area per head group (83 $Å^2$) than in the equilibrated L_α bilayer discussed previously. Although one might thus expect a pure single leaflet monolayer to form, there are two reasons for this not being the case. Firstly, the interaction potentials for the CG model are soft compared to their atomistic counterparts. This gives rise to enhanced diffusion as discussed below and makes it easy for lipid molecules to slide past one another. Once a lipid finds itself out of direct contact with water, it can orient itself to form a partial lipid bilayer. The driving force for it to go back into the monolayer

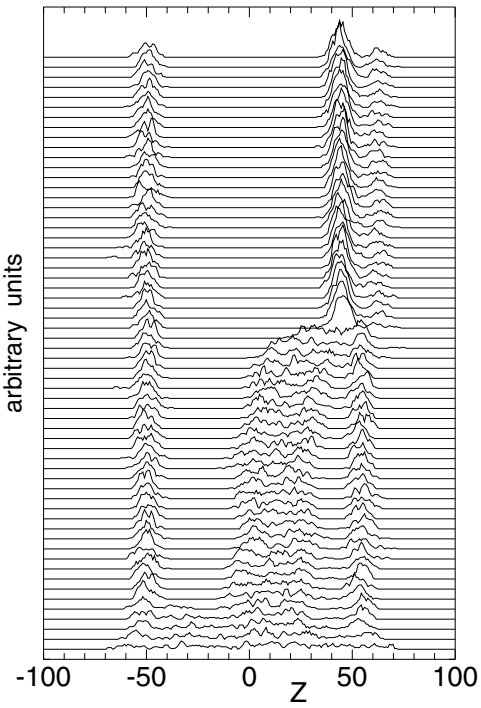

Figure 9. Evolution of the lipid head group density throughout the self-assembly simulation. The head group electron density is projected onto the axis normal to the air/water interface at 60 equally spaced intervals over the 2 ns simulation. The system quickly assembles into two interfacial monolayers and a micelle in the bulk water environment. This micelle then diffuses towards and fuses with one of the Langmuir monolayers. The formation of a partial outer leaflet should be noted.

is weak and the barrier to doing so is large. Secondly, the simulation is run for a long time. Inter-leaflet flips are rare events but they will eventually occur. The soft interaction potentials enhance the effect of thermal fluctuations. The leaflet flipping events are currently being studied in more detail.

3.3.2. Lipid translation in the self-assembled monolayers. We complete the dynamic picture of the motions of CG DMPC monolayers by comparing the motion of the bilayer lipids with those in the equilibrated self-assembled monolayers. The plot of the lateral diffusion of CG lipids after self-assembly is shown in figure 10. The leaflet with fewer lipids exhibits the fastest self-diffusion coefficient, as expected, with $D_{mono} = 52 \times 10^{-6}$ cm^2 s^{-1}. The area per head group in this leaflet is 233 Å^2, which shows how loose the packing is in this monolayer. The diffusion coefficient for the other monolayer is $D_{mono} = 18 \times 10^{-6}$ cm^2 s^{-1}, and the area per head group is 83 Å^2. This coefficient lies in between the coefficient for the bilayer and that of the dilute monolayer. This result is consistent with the ordering of the area per head group and therefore the packing in each of the subphases. In addition, one expects the diffusion in the monolayer to be faster than that in the bilayer because there is an interaction with the tails of lipids in the opposite leaflet in the case of the bilayer. The present model seems to reproduce transport properties consistently across different lipid concentrations.

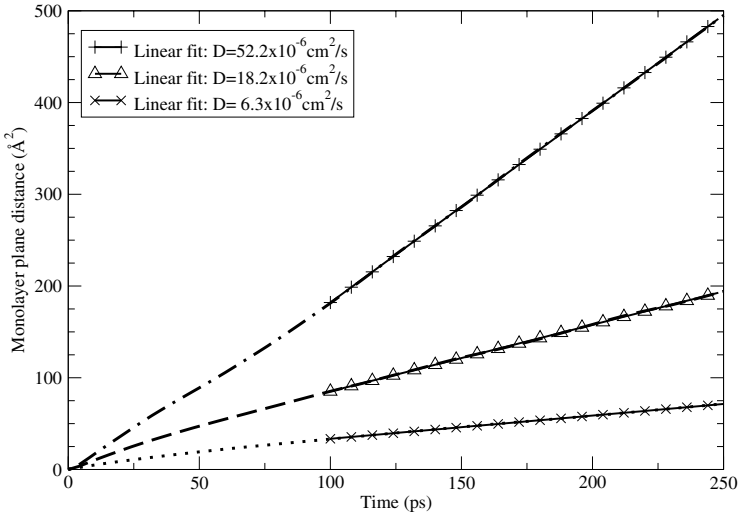

Figure 10. The two-dimensional MSD for the self-diffusion of the lipids with an area of 233.3 Å^2 per head group in a lipid monolayer (— · —), 83.1 Å^2 per head group in a lipid monolayer (— — —), and 70 Å^2 per head group in a bilayer (· · · · · ·). The fits are made from 100 to 250 ps, and τ in equation (1) is 250 ps.

4. Conclusions

The overall motion of the CG lipids is one to two orders of magnitude faster than the AA formulation. However, the more efficient simulation scheme adds an additional reduction in computational cost by two to three orders of magnitude. Our finding is that the components of the CG and AA lipids follow similar trends overall and there is agreement in terms of the relative timescales of translational dynamics. The rotational dynamic constants in the CG model maintain a qualitative description of the AA molecule, except for the case of the PN vector. The PN vector rotation anomaly is due to the coarse graining of the slow hydrogen bonding dynamics at the lipid/water interface. On average, the lipid PN vector is essentially parallel to the bilayer surface. The CG model for DMPC/water systems allows access to timescales that were previously accessible only at immense computational cost for MD simulations.

It is now possible to routinely carry out computer experiments of self-assembly with the present CG model. In the chosen system the molecules spontaneously self-assemble into monolayers at each of the two air/water interfaces. The most interesting observation from the self-assembly of the monolayers is the fusion mechanism of a micelle with one of the monolayers. The timescale of the entire simulation is effectively 200 ns. Ongoing work to further characterize the systems presented here will involve studying the large-scale thermal fluctuation modes of a bilayer along with inter-leaflet flipping events. The ease of computation using the CG models should allow calculation of the surface tension for Langmuir monolayers and other properties.

It has been demonstrated that the present CG model can provide insight into the dynamical behaviour of mesoscale phases. Further improvement of the model is currently under way to address some of its shortcomings. From the present and previous results, we see that this type of approach can be a useful tool for investigation of mesoscale phenomena involving membranes and membrane-bound species.

Acknowledgments

The authors would like to thank Ivaylo Ivanov for several helpful suggestions, and the referees for their useful comments and insights, all of which greatly improved the manuscript.

References

[1] Cevc G (ed) 1993 *Phospholipids Handbook* (New York: Dekker)
[2] Blume A 1993 *Phospholipids Handbook* (New York: Dekker) ch 13, p 10 016
[3] Gennis R B 1989 *Biomembranes: Molecular Structure and Function* (Berlin: Springer)
[4] Tarek M, Tu K and Tobias M L 1999 *Biophys. J.* **77** 964
[5] Essmann U and Berkowitz M L 1999 *Biophys. J.* **76** 2081
[6] Pastor R W and Feller S E 1996 *Biological Membranes* ed J K Merz and B Roux (Boston, MA: Birkhäuser) pp 4–29
[7] Gil T, Ipsen J H, Mouritsen O G, Sabra M C, Sperotto M M and Zuckermann M J 1998 *Biochim. Biophys. Acta* **1376** 245
[8] Lyubartsev A P and Laaksonen A 1995 *Phys. Rev.* E **52** 3370
[9] McGreevy R L and Pusztai L 1988 *Mol. Simul.* **1** 359
[10] Shelley J C, Shelley M Y, Reeder R C, Bandyopadhyay S and Klein M L 2001 *J. Phys. Chem.* B **105** 4464
[11] Lopez C F, Moore P B, Shelley J C, Shelley M Y and Klein M L 2002 *Comput. Phys. Commun.* **147** 1
[12] Moore P B, Lopez C F and Klein M L 2002 *Biophys. J.* **81** 2484
[13] Shelley J C, Shelley M Y, Reeder R C, Bandyopadhyay S, Moore P B and Klein M L 2001 *J. Phys. Chem.* B **105** 4464
[14] Shelley J C *Modified Coarse Grain Parameters for MD Simulations in the NPT Ensemble* available through the web at www.cmm.upenn.edu
[15] Frenkel D and Smit B 1996 *Understanding Molecular Simulation* (San Diego, CA: Academic)
[16] Tuckerman M E and Martyna G J 2000 *J. Phys. Chem.* B **104** 159
[17] Martyna G J, Klein M L and Tuckerman M 1992 *J. Chem. Phys.* **97** 2635
[18] Nagle J F and Tristram-Nagle S 2000 *Biochim. Biophys. Acta* **1469** 159
[19] Husslein T, Newns D M, Pattnaik P C, Zhong Q, Moore P B and Klein M L 1998 *J. Chem. Phys.* **109** 2826
[20] Lindahl E and Edholm O 2000 *Biophys. J.* **79** 426
[21] Feller S E, Pastor R W, Rojnuckarin A, Bogusz S and Brooks B R 1996 *J. Phys. Chem.* **100** 17 011
[22] Tobias D J 2001 *Curr. Opin. Struct. Biol.* **11** 253
[23] Tieleman D P, Marrink S J and Berendsen H J C 1997 *Biochem. Biophys. Acta* **1331** 235
[24] Venable R M, Brooks B R and Pastor R W 2000 *J. Chem. Phys.* **112** 4822
[25] Walser R, Huenenberger P H and van Gunsteren W F 2001 *Prot. Struc. Funct. Gene.* **44** 509
[26] Wang Z and Holm C 2001 *J. Chem. Phys.* **115** 6351
[27] Baker N A, Huenenberger P H and McCammon J A 1999 *J. Chem. Phys.* **110** 10 679
[28] Bogusz S, Venable R M and Pastor R W 2001 *J. Phys. Chem.* B **105** 8312
[29] Marrink S J, Tieleman D P and Mark A E 2000 *J. Phys. Chem.* B **104** 12 165
[30] Marrink S J, Lindahl E, Edholm O and Mark A E 2001 *J. Am. Chem. Soc.* **123** 8638
[31] Israelachvili J and Wennerstrom H 1992 *J. Phys. Chem.* **96** 520